Journal of Renewable Materials

Tech Science Press

DOI: 10.32604/jrm.2022.021214

ARTICLE

Utilization of Low-Alkalinity Cementitious Materials in Cemented Paste Backfill of Gold Mine Tailings

Jiamao Li[1,2,*], Chuimin Zhang[1], Lin Li[1], Chuangang Fan[1,*], Zhaofang He[3] and Yuandi Qian[3]

[1]School of Materials Science and Engineering, Anhui University of Technology, Maanshan, 243032, China

[2]Key Laboratory of Green Fabrication and Surface Technology of Advanced Metal Materials, Ministry of Education, Maanshan, 243002, China

[3]China MCC17 Group Co., Ltd., Maanshan, 243000, China

[*]Corresponding Authors: Jiamao Li. Email: agdjiamaolee@126.com; Chuangang Fan. Email: chgfan67@163.com

Received: 01 January 2022 Accepted: 18 February 2022

ABSTRACT

The purpose of this paper was to explore the possibility of using low-alkalinity cementitious materials as binders, in which ground blast furnace slag and fly ash acted as a partial replacement of ordinary Portland cement, and $CaSO_4$, Na_2SO_4, and CaO were used as a sulfate activator and alkali-activated additives, to solidify gold mine tailings for preparation of a green, inexpensive cemented paste backfill (CPB). For this target, the effects of cement/tailings ratio, superplasticizer dosage, solid content, tailings fineness on the mechanical properties of the CPB were investigated. Additionally, the hydration mechanism of the CPB was analyzed based on X-ray diffraction and scanning electron microscopy results. The results showed that the fluidity of the CPB slurry could be improved by adding polycarboxylic acid superplasticizer. The unconfined compressive strength (UCS) of the CPB specimens was increased with the increase of cement/tailings ratio and solid content. Under the same experimental conditions, the 28 d UCS of the CPB specimens was 3.8~4.9 times higher than that of ordinary Portland cement. The softening coefficient of the CPB specimens was increased with the increasing cement/tailings ratio, ranging from 0.83 to 0.92. The shrinkage rate of the CPB specimens was decreased from 0.70% to 0.54% with the increase of cement/tailings ratio from 1:12 to 1:4. The UCS of the full tailings CPB was the highest, followed by the fine tailings CPB specimens, and the UCS of the coarse tailings CPB specimens was the lowest. The low-alkalinity binder was proved to be a promising material to improve the engineering performances of the CPB. The optimal mixing ratio is 1:6 cement/tailings ratio, 0.15 wt% superplasticizer dosage, and 70 wt% solid content. Prepared by this mixing ratio, the UCS values of the CPB after 3, 7, and 28 d curing ages reached 1.85, 5.87, and 9.16 MPa, respectively, which were suitable as CPB for the Zhaoyuan gold mine in terms of strength requirements.

KEYWORDS

Cemented paste backfill; blast furnace slag; fly ash; engineering properties; waste utilization

1 Introduction

Nowadays, mining industry has played an important role in the development of global economy, providing a variety of raw materials including a series of industrial substances gold, silver, copper, and

iron for practical applications. Compared with other primary ores, gold ore has a relatively low grade. Therefore, a large number of gold tailings are produced during mining and dressing process. But they cannot be efficiently utilized and have to be stored in surface facilities such as dams, ponds, and embankments. Till now, the stockpiles of gold tailings in the world have been up to 14,000 million tons [1]. According to the estimating, more than 20 million tons of gold tailings have been produced annually in China, leading to 12,000 tailings ponds [2,3]. Tailings ponds not only destroy limited land resources but also bring air pollution, water pollution, and even serious accidents. For example, a disaster that happened in a tailing pond located in Minas Gerais of Brazil led to at least 235 persons death and 35 persons missing, and several buildings being damaged [1]. Therefore, it is extremely urgent to solve the problem of the storage and disposal of gold tailings.

Four approaches have been developed as solutions to reduce adverse effects on the environment, human life, and health posed by the massive accumulations of gold tailings: (1) returning green manure in gold tailings [4,5], (2) comprehensive recovery of valuable elements from gold tailings [6–9], (3) production of building materials using gold tailings [10–14], and (4) utilization of gold tailings based on cemented paste backfill (CPB) technology [15–21]. For the management of process gold tailings, naturally, CPB technology is believed to be one of the most effective practical approaches due to its significant technical, economic, and environmental merits such as mitigating the potential environmental influence caused by hazardous mill tailings, providing a safe work environment for underground mining, and reducing the mill tailings disposal and rehabilitation costs [22,23]. The CPB technology is booming development in mine industry and related research fields all over the world as an alternative and innovative for disposal of mine tailings.

In the past few years, the exploration of new backfill materials for the CPB technology has become one of the hot spots rapidly in China and other industrialized countries such as America, Canada, and Australia. CPB is composed mainly of mine tailings, cementitious materials (or binders), mixing water, and minerals admixtures. The binder type and its proportion to other components in the CPB should be appropriately designed for achieving favorable mechanical properties. Ordinary Portland cement (OPC) was the most widely used binder in early reports due to its good binding performance. Ercikdi et al. [24] studied the effects of OPC, Portland composite cement (PCC), and sulphate resistant cement (SRC) on the engineering properties and microstructure of the CPB and found that the binder type, dosage, and water-to-cement ratio had significant influences on the short-term and long-term engineering properties. Subsequently, an investigation [25] demonstrated that sulfate and temperature were two crucial factors for the design of CPB structure using OPC as binder. Recently, Chen et al. [26] developed a new cemented paste backfill, which was composed of iron ore tailings, 42.5 OPC, and three mineral additions according to alkali-activated theory. Based on the mixture design modeling approach, they modeled the influences of cement, lime, and silica fume on the spread and mechanical properties of the CPB. Finally, optimal mix proportions were obtained successfully. These results have witnessed that the OPC content has a remarkable effect on the mechanical properties of the CPB. However, the OPC is not an ideal candidate for the fine particle mine tailings since the mine tailings are becoming finer and finer and even the proportion of the fine particle with less than 20 μm is significant increased [2,27]. In this case, in order to enhance the mechanical strength, a large volume of OPC is introduced to the CPB unavoidably, leading to the increase in the filling cost greatly. Therefore, exploring new-type of binder materials with low cost and high efficiency to replace OPC partially has been a hot issue for practical application.

On this background, in the past few years, continuous research on the binder materials containing industrial waste products such as ground granulated blast-furnace slag, fly ash, lithium slag, phosphogypsum, silica fume has been conducted [17,28–35]. Marvila et al. [28] investigated the fresh and rheological properties of alkali mortars activated by blast furnace slag (BFS) and found that the mortars containing between 2.5% and 7.5% of sodium exhibited the same rheological behavior as

cementitious mortars. Furthermore, their latest discovery [29] reveals that the utilization of ground blast furnace slag (GBFS) is a viable alternative for the production of activated alkali cements that is a potential substitute for OPC. Li et al. [30] studied the feasibility of using fly ash–slag-based binder for mine backfilling and established an optimal composition of the CPB. Using lithium slag and fly ash as the main components of binder for cemented fine tailings backfill, a feasibility investigation was carried out by He et al. [31]. The obtained unconfined compressive strength values could satisfy the strength requirements of backfill to support the surrounding rock of stopes of Yinshan lead-zinc mine. Sun et al. [34] prepared a new-type CPB using mine tailings as aggregate, slag and silica fume as binder, sodium hydroxideas activator and explored its strength development mechanism. They found that C-S-H gels and Mg-Al type layered double hydrotalcites generated in the CPB were responsible for dense structure and improved strength. Moreover, these reports indicated that alkali-activated binders were promising alternatives for production of new-type CPB.

More recently, Zheng et al. [36] experimentally studied the properties of reactive MgO-activated slag (MAS)-waste gypsum (WG) plasters and MAS-WG-CPB of lead–zinc mine tailings and reported that the utilization of MAS-WG as binders to solidify and stabilize sulphide-rich tailings had stable long-stage compressive strengths in 180 days due to the low-alkalinity solution in MAS-WG-CPB. Herein, from the viewpoint of alkalinity of the binders, we investigate the feasibility of blending BFS, fly ash, and 42.5 level OPC with a certain amount of chemical additives $CaSO_4$, Na_2SO_4, and CaO to substitute conventional clinker with a certain ratio of gold tailings for manufacturing a green and low-cost new-type CPB. The effects of cement/tailings ratio, superplasticizer content, solid content, tailings fineness on the mechanical properties of the CPB were investigated. In addition, the hydration mechanism of the CPB was analyzed based on X-ray diffraction and scanning electron microscopy results.

2 Materials and Methods

2.1 Materials

2.1.1 Gold Tailings

Three types of gold tailings were used in the present work, including total tailings (TT), coarse tailings (CT), and fine tailings (FT), which were sampled from the Zhaoyuan Gold Mine located at Shandong Province of China. The particle size distribution of these gold tailings was measured by a laser particle size analyzer (Rise-2006, Jinan Runzhi Technology Co., Ltd., China) and the result is shown in Fig. 1. Table 1 also provides the particle size parameters (PSP) of the gold tailings used in the present work. The TT and FT exhibit similar particle size distributions whose average particle sizes are 14.84 and 11.91 μm, respectively. Moreover, the proportions of the fine particles with less than 20 μm in TT and FT are 72.1% and 81.5%, respectively. These data significantly differ from those on the CT (average particle size is about 144.36 μm, and the fine particles with less than 20 μm can be negligible). The TT with fine particles (<20 μm) content of above 60% can be sorted as fine size tailings with a good flow transport performance to form a paste. Correspondingly, the FT can be sorted as ultra-fine tailings. However, its strength is always poor due to a high water/cement ratio. The chemical composition of gold tailings determined by XRF is shown in Table 2. As can be seen, SiO_2 and Al_2O_3 are the main chemical ingredients of gold tailings. In general, high SiO_2 content in gold tailings will reduce the consolidation performance of consolidating body to a certain extent since quartz is an inert material [37]. As a result, it is necessary to increase the cement/tailings ratio in the CPB for ensuring the consolidation strength of consolidating body.

2.1.2 Binders and Chemical Activators

The main raw materials used for the binder of CPB in the experiment contained ground blast furnace slag (GBFS), fly ash (FA), and ordinary Portland cement (OPC), and their chemical compositions are displayed in Table 2. It is well known that the GBFS and FA are mainly composed of glassy phases CaO-SiO_2-Al_2O_3-MgO.

The GBFS taken from Magang Jiahua New Building Materials Co., Ltd. in Anhui Province of China includes 37.70% CaO, and the percentage of CaO-SiO_2-Al_2O_3-MgO is as high as 95.6%. Contrasted to the GBFS, the FA provided by Maanshan No. 2 power plant in Anhui province of China contains merely 3.42% CaO, and the amount of CaO-SiO_2-Al_2O_3-MgO is 92.49%. Thus, it can be categorized as a Class F fly ash (the total content of SiO_2, Al_2O_3, and $Fe_2O_3 \geq 70\%$) that has pozzolanic properties according to ASTM C618-19. From Table 2, the specific surface area of GBFS and FA was 3100 cm^2/g and 7650 cm^2/g, respectively.

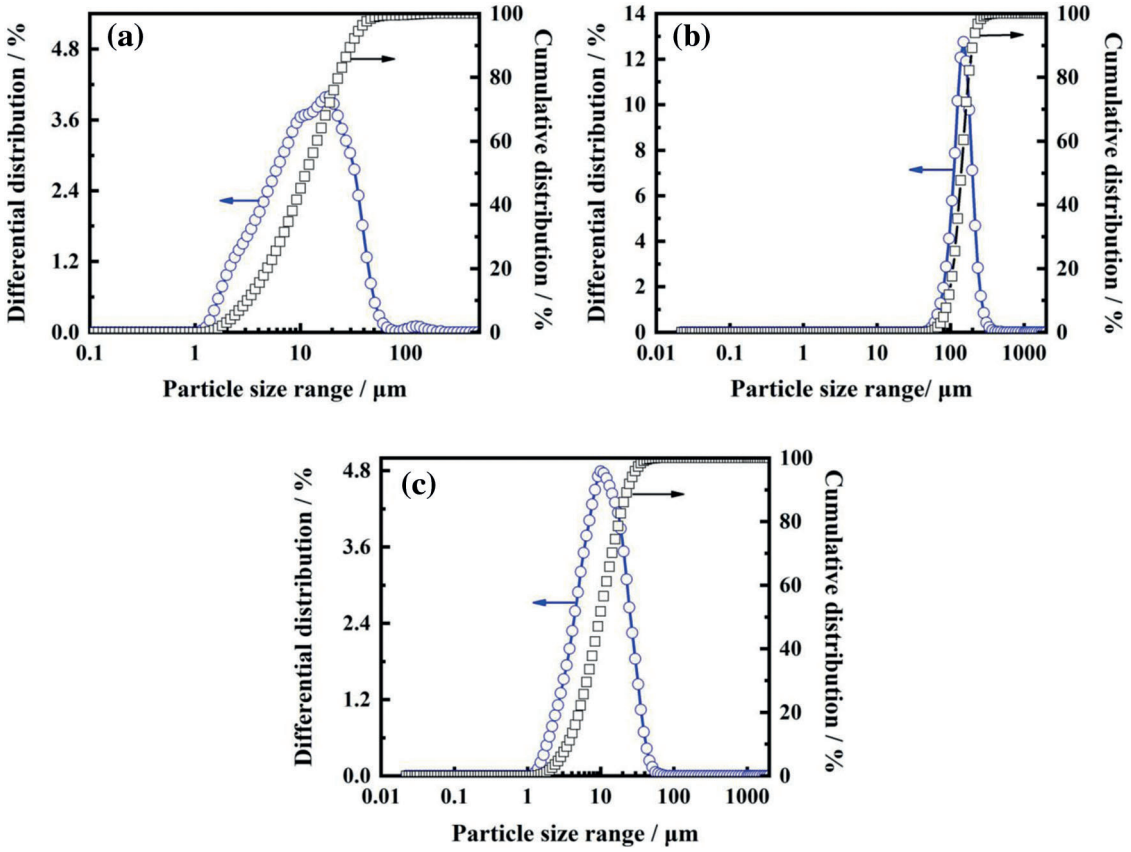

Figure 1: Particle size distribution curves of the gold tailings: (a) Total tailings; (b) Coarse tailings; (c) Fine tailings

Table 1: PSP of the gold tailings used in the present work

	PSP							
Gold tailings	D_3/μm	D_{10}/μm	D_{50}/μm	D_{90}/μm	D_{97}/μm	D_{av}/μm	S/V/(m^2/cm^3)	pH
TT	3.13	3.45	11.31	30.33	38.95	14.84	0.48	6.62
FT	2.26	3.54	9.75	23.35	29.73	11.91	0.61	6.45
CT	73.78	92.33	139.93	200.40	236.34	144.36	0.05	6.81

Table 2: Chemical composition (wt%) and specific surface area (cm^2/g) of main raw materials

Raw materials	SiO_2	Al_2O_3	K_2O	Na_2O	CaO	Fe_2O_3	MgO	TiO_2	SO_3	Specific surface area (cm^2/g)	LOI (wt%)
Gold tailings	70.14	17.30	4.95	3.78	1.87	0.72	0.54	–	–	–	3.02
GBFS	32.90	17.09	–	0.89	37.70	0.66	7.91	1.60	1.25	3100	1.35
FA	59.15	29.11	2.28	0.67	3.42	3.71	0.81	0.35	0.82	7650	2.15
OPC	20.85	5.95	1.10	0.36	61.24	2.60	1.25	–	2.85	3580	3.62

The OPC was 42.5 grade cement (equal to CEMII 42.5N) based on the Chinese standard GB175-2007 and was purchased from Conch Cement Co., Ltd. in Anhui Province of China. Its main chemical ingredients are CaO, SiO_2, and Al_2O_3. Its main phase compositions are tricalcium silicate (C_3S), dicalcium silicate (C_2S), and tricalcium aluminate (C_3A). The measured specific surface area value is 3580 cm^2/g.

The chemical activators of calcium sulfate dihydrate ($CaSO_4 \cdot 2H_2O$, ≥99.0 mass%), sodium sulfate (Na_2SO_4, ≥99.0 mass%), and calcium oxide (CaO, ≥96.0 mass%) were purchased from Sinopharm Chemical Reagent Co. Ltd. of China. These chemicals could be used directly in the experiment. Polycarboxylic superplasticizer was produced by Chenqi Chemical Technology Co., Ltd. in Shanghai of China. In addition, tap water was used in this work.

2.1.3 Preparation of the Low-Alkalinity Binder (BLA)

The BLA was prepared using GBFS, FA, 42.5 grade OPC, sodium sulfate, calcium oxide, and calcium sulfate as raw materials. The mix ratio of the BLA is shown in Table 3. It was the optimal one that was obtained by our previous work (not published). Firstly, these raw materials were weighted at a certain ratio and stirred uniformly in a double spiral mixer for about 10 min. Then, they were transferred to a horizontal ball mill and ball-milled with stainless steel ball for about 1 h. According to the horizontal vibration method, the as-prepared cementitious material was leached and the leaching solution was extracted based on the Chinese standard HJ 557–2009. The pH value of the leaching solution was determined by a digital display pH–meter (PHS-25, Shanghai INESA Scientific Instrument Co., Ltd., China), and the measured pH value was 9.8. Finally, the low-alkalinity cementitious material was successfully prepared.

Table 3: Mix ratio of BLA (wt%)

GBFS	FA	OPC	Calcium oxide	Calcium sulfate	sodium sulfate
65	14	10	6	4.5	0.5

2.1.4 Preparation of the CPB Specimens

Firstly, a chosen dosage (0.05%–0.2% by mass of gold tailings slurry) of superplasticizer was added into the gold tailings slurry with a certain solid content under the condition of continuous mechanical stirring in a double spiral mortar mixer for about 5 min. Then, the prepared BLA was thoroughly mixed to the above slurry together with a certain amount of tap water until a homogeneous paste was obtained. Finally, the CPB mixture was poured into 40 mm × 40 mm × 160 mm mortar moulds. Excessive water in the specimens was flushed out from the seam between baseboard and broadsides of the mortar moulds. Then, these specimens were sealed and placed into a humidity chamber set at (20 ± 2)°C, and relative humidity of more than 95% for curing. According to the Chinese standard JGJ/T 70-2009, the CPB specimens with

different curing ages were conducted to the UCS tests. The mix proportions are shown in Table 4. In addition, a reference experiment that the gold tailings were cemented by 42.5 grade OPC alone was also employed. Table 5 lists its mix proportion. In this work, the effects of gold tailing type, solid content, cement/tailings ratio, dosage of superplasticizer, and binder type on the engineering properties of the CPB specimens were studied by the single factor experiment.

Table 4: Mix proportions of the CPB sample using BLA as binder

Series	Gold tailings	Solid content (wt%)	Cement/tailings ratio	Dosage of PS (wt%)	Curing age (d)
SS	TT	70	1:6	0	3, 7, 28
				0.05	
				0.10	
				0.15	
				0.20	
SR	TT	70	1:4	0.15	3, 7, 28
			1:6		3, 7, 28
			1:8		3, 7, 28
			1:10		3, 7, 28
			1:12		3, 7, 28
SC	TT	60	1:6	0.15	3, 7, 28
		65			3, 7, 28
		70			3, 7, 28
ST	TT	65	1:6	0.15	3, 7, 28
	CT				3, 7, 28
	FT				3, 7, 28

Table 5: Mix proportion of the CPB sample using OPC as binder

Series	Gold tailings	Solid content (wt%)	Cement/tailings ratio	Dosage of PS (wt%)	Curing age (d)
SO	TT	70	1:6	0.15	3, 7, 28
			1:8		
			1:10		
			1:12		

2.2 Test Methods

2.2.1 Unconfined Compressive Strength (UCS)

It is widely accepted that UCS is one of the most essential performances of cementitious paste backfill in order to ensure its quality [36]. In this study, according to the standard for test method of mechanical properties on ordinary concrete (GB/T 50081-2002), the UCS tests were performed on the samples with various curing times (3, 7, and 28 d) by an electronic universal testing machine (WDW-30, Jinan Metus Testing Technology Co., Ltd., China) with a maximum capacity of 30 kN. Before tests, the actual

compression area of each sample facing the loading direction was measured and the UCS value could be obtained based on Eq. (1):

$$\sigma = \frac{F}{A} \tag{1}$$

where σ, F, and A were the UCS (MPa), the failure load (kN), and the compression area (cm^2) of the sample facing the loading direction, respectively.

2.2.2 Slump Test

The rheological property of the CPB slurry is a crucial index to assess transportation feasibility. The slump value is commonly considered as a key factor to reflect the flowability of high-concentration backfill materials. It has been found that a backfill slurry with a slump value of 190–270 mm can be transported to a stope by self-flowing via its gravity successfully [32,38]. However, the harshly required slump value from our cooperative enterprise was 275 mm. Herein, the slump value in this present work was controlled at approximately 275 mm. According to the Chinese standard GB/T 50080-2002, the slump tests were conducted and repeated three times, and the slump value was achieved using the average value of the three test results. The detailed operating instruction can be referred to previous literature [39].

2.2.3 Softening Coefficient Test

For the softening coefficient test, the CPB specimens were sealed and placed into a humidity chamber set at (20 ± 2)°C and relative humidity of more than 95% for 28 d curing time. The softening coefficient K was calculated using Eq. (2) based on the British Standard EN 12859-2008:

$$K = \frac{f}{F} \tag{2}$$

where f and F represented the residual compressive strength (MPa) of the 28 d cured CPB specimen after immersing in water for 24 h and the compressive strength (MPa) of the 28 d cured CPB in the dry air, respectively. Three specimens from each mix were prepared and the softening coefficient value was obtained by averaging the three test results.

2.2.4 Shrinkage Test

The shrinkage performance measurement of the CPB specimen was conducted based on the Chinese standard JC/T 603-2004. The shrinkage rate S of the CPB specimens at 28 d curing age was calculated according to the Eq. (3):

$$S = \frac{L_0 - L}{L} \times 100\% \tag{3}$$

where L_0 and L were the initial length (mm) of the CPB specimen at 3 d curing age and the length (mm) of the CPB specimen at 28 d curing age, respectively. Clearly, a positive S value represents a contraction while a negative S value indicates an expansion.

2.2.5 XRD and SEM Analysis

Phase composition of the hydration products was identified by a powder X-ray diffractometer (XRD, D8 Advance, Bruker, Germany) using Cu Kα radiation with a 2θ scanning range of 10–80° and a scanning speed of 4 °/min. Before XRD identification, the samples that have been subjected to the UCS test were stored into ethanol for 3 days to terminate the hydration process and were dried for about 8 h to obtain the constant weight. Fragments of the crushed samples were coated with gold, and then the micromorphology of the fragments was observed by a scanning electron microscopy (SEM, JSM6490LV, Tokyo, Japan).

3 Results and Discussion

3.1 Cementitious Characteristics of OPC and BLA Binders

The UCS values of the CPB specimens prepared by different binders with a solid content of 70 wt% are shown in Fig. 2. It is seen that the addition of OPC or BLA to the gold tailing slurry can improve the UCS at 3, 7, and 28 d curing ages. Moreover, the UCS value is increased with the increase of cement/tailings ratio, indicating OPC and BLA have the ability to cement the total tailings. Except for 1:6 cement/tailings ratio, the BLA specimens with different cement/tailings ratios exhibit higher UCS values at 3 d curing age than those of the SO specimens, as shown in Fig. 2a. These results imply that the OPC content has to be increased to satisfy the early-term strength requirement during filling processing. Correspondingly, the cement filling cost is increased while the fluidity of tailings slurry is reduced. As far as the middle-late-term strength is considered, as illustrated in Figs. 2b and 2c, the UCS values of the specimens with BLA are outstanding higher than the SO specimens. For example, after being cured for 28 d, the specimens with BLA have the UCS values of 3.24, 4.26, 5.55, and 8.25 MPa, respectively. Comparatively speaking, the UCS values of the OPC specimens at the same curing age are 0.66, 0.88, 1.41 and 2.17 MPa, respectively. It is clear that the UCS values of the specimens with BLA increase 3.91, 3.84, 2.94, and 2.80 times, respectively, as revealed in Fig. 2d.

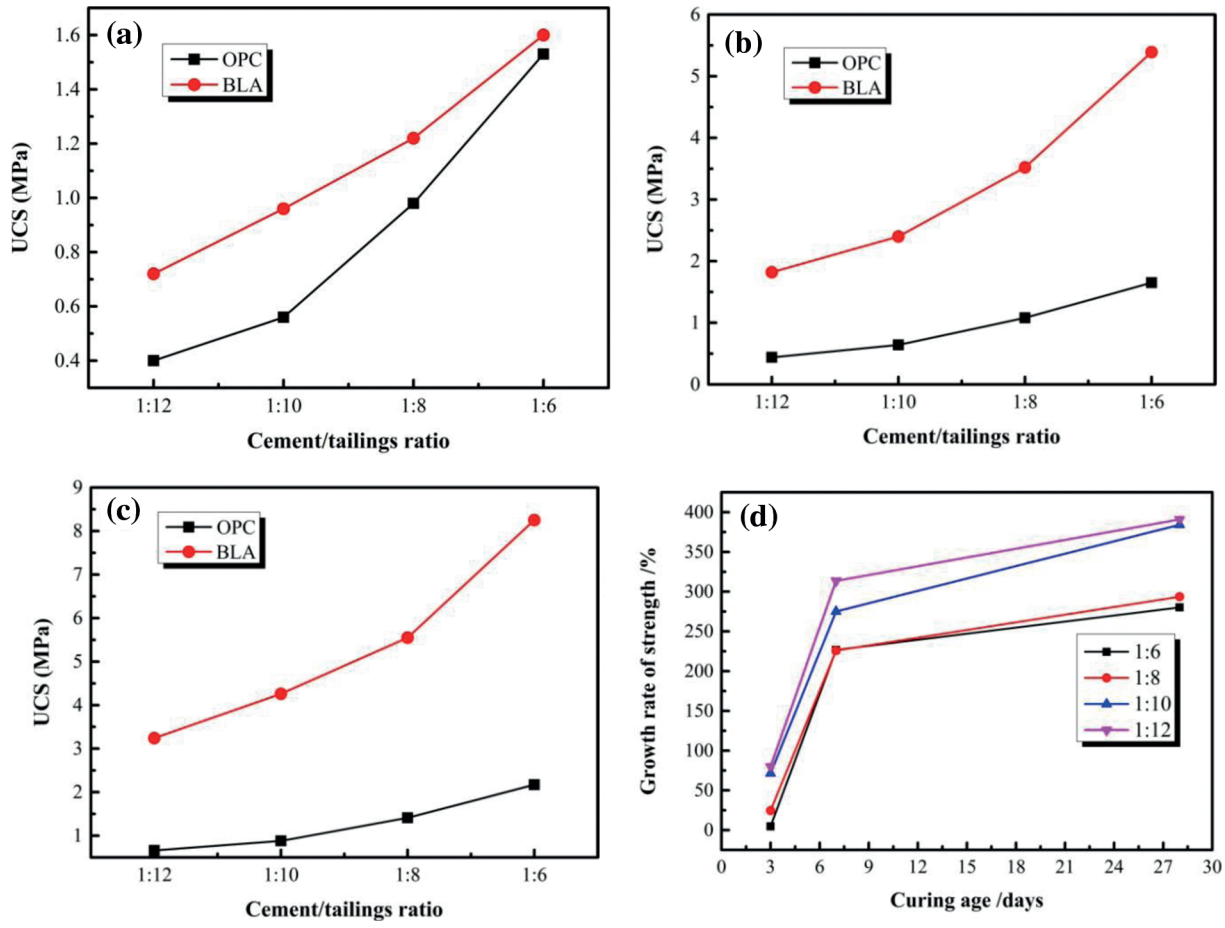

Figure 2: UCS values of the CPB specimens with various curing ages: (a) 3 d, (b) 7 d, (c) 28 d, and growth rate of strength of the CPB specimens by substituting BLA for OPC (d)

The increase in the UCS should be attributed to the partial replacement of OPC by GBFS and FA. On the one hand, the FA with finer particles in the BLA is beneficial to form a denser structure, namely the "filling effect" of FA can improve the strength of the specimens. As we know, reduced porosity in the hardened materials is a key factor to obtain high strength. On the other hand, the active components in the GBFS and FA will exhibit a pozzolanic activity by secondary hydration reaction due to the excitation effect of chemical activators such as Na_2SO_4 and $CaSO_4$. More stable hydration products generated are helpful in enhancing the strength of the specimens.

Fig. 3 shows the slump test results of the tailings slurry prepared by OPC and BLA separately with different cement/tailings ratios. As can be seen, the slump values decline when the cement/tailing ratio increases from 1:12 to 1:6 regardless of binder type, indicating high solid content has an adverse influence on the flowability of the tailing slurry. Compared with the addition of OPC alone, the addition of BLA noticeably reduces the slump value. However, all the slump values are acceptable to meet the fluidity requirements of the gold mine backfill system of our cooperative enterprise. Hence, the disadvantageous influence on the transportation properties of the tailings slurry with BLA can be ignored.

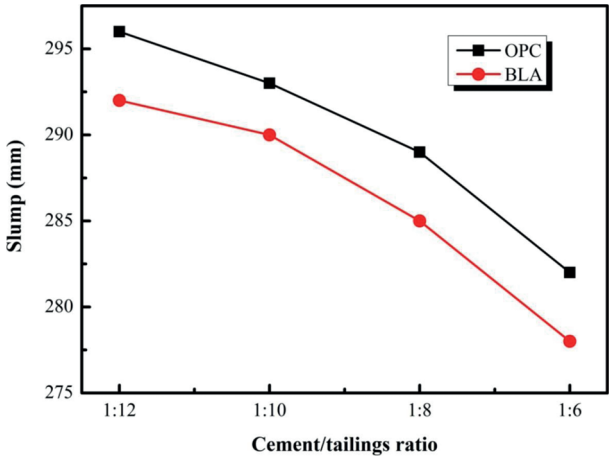

Figure 3: Slump test results of the tailings slurry prepared by OPC and BLA separately

3.2 Effects of Superplasticizer Dosage on the Performances of CPB

The utilization of superplasticizer is critical to ensure the workability of CPB. Furthermore, the superplasticizer dosage has a profound effect on the strength and fluidity properties of CPB. Herein, a series of UCS and slump tests were conducted in this study. Fig. 4 presents the effect of superplasticizer dosage on the slump value of the filling slurry with BLA at a fixed solid content of 70 wt% and cement/tailings ratio of 1:6. It is clear that the dosage of superplasticizer has a pronounced influence on the slump value of the filling slurry. A tendency of a significant increase in the slump value of the tailings slurry is found with increasing superplasticizer dosage up to 0.20 wt%. The slump value increases from 260 to 290 mm when the superplasticizer dosage increases from 0 wt% to 0.20 wt%. This increase in the slump value can be associated with the surface characteristics of polycarboxylic superplasticizer such as its low absorptivity. As the superplasticizer dosage increases from 0 wt% to 0.20 wt%, more and more void filled water in the slurry is compelled to remove from the void so that the slump value of the CPB mixture increases. The filling slurry needs to have good flowability to avoid pipe blockage in mine filling process. Meanwhile, it also possesses desired cohesion and water retention so that the filling slurry will not be layered or bled.

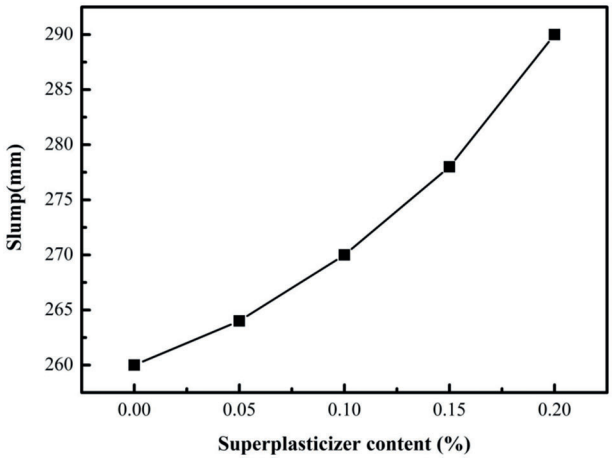

Figure 4: Effect of superplasticizer dosage on the slump value of the filling slurry with BLA

Fig. 5 demonstrates the effect of superplasticizer dosage on the UCS value of the CPB specimens with various curing ages. As shown in this figure, the UCS value of the CPB specimens increases gradually as the superplasticizer content increases from 0 wt% to 0.15 wt%, and decreases at 0.20 wt% superplasticizer content regardless of curing age. In the current work, the 28 d UCS was considered as ultimate strength, the UCS development ratio was obtained, as displayed in Table 6. It is obvious that the 7 d UCS development rate (ranging from 56.5% to 65.3%) is higher than the 3 d UCS development rate (ranging from 10.1% to 19.4%). Significantly, the SS sample with 0.20 wt% superplasticizer exhibits such low UCS values, which is unsuitable to the requirement of mine filling intensity. Based on the comprehensive analysis of the slump and the UCS, the optimal dosage of superplasticizer should be 0.15 wt%, accounting for the mass of mine slurry.

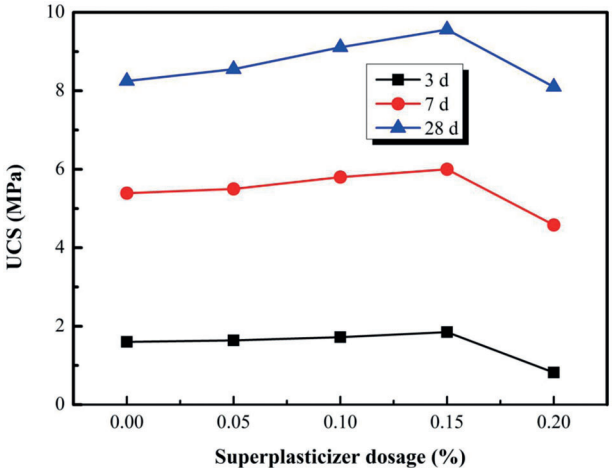

Figure 5: Effect of superplasticizer dosage on the UCS value of the CPB specimens with various curing ages

Table 6: 3 and 7 d UCS development rate of the CPB specimens

Superplasticizer dosage/wt%	3 d UCS development rate/%	7 d UCS development rate/%
0	19.4	65.3
0.05	19.2	64.3
0.10	18.9	63.7
0.15	19.4	62.8
0.20	10.1	56.5

3.3 Effects of Cement/Tailings Ratio on the Performances of CPB

It is believed that the cement/tailings ratio of the CPB mixture has an outstanding impact on its engineering performances for the CPB technology used in underground mines. Figs. 6–8 demonstrate the effects of cement/tailings ratio on the UCS, softening coefficient, and shrinkage ratio of the SR series samples, respectively. On the one hand, as presented in Fig. 6, the UCS value of the SR samples obviously increases with an increase in the curing age for a fixed cement/tailings ratio. For instance, the UCS value of the SR samples with a cement/tailings ratio of 1:6 at 3 d curing age is merely 1.85 MPa. By comparison, the UCS values of the same composition at 7 and 28 d curing ages can be up to 5.87 and 9.16 MPa, respectively. It is also found in Table 7 that the growth rates of the UCS for the SR samples after cured 3 d are around 20%. However, for the SR samples with 7 d curing age, the growth rates of the UCS exceed 50%. On the other hand, the UCS value of the SR samples increases with the increase of cement/tailing ratio. The reason is that the amount of hydration products generated in the hydration process is increased when the cement/tailings ratio increases. Correspondingly, the UCS of the sample is improved. Nevertheless, the degree of increase of 3 d UCS is not as obvious as those of 7 d UCS and 28 d UCS. The curing age has made an even stronger influence on the UCS than the cement/tailings ratio for the SR samples with early-term hydration. In view of the BLA binder used in the study, the secondary hydration reaction will be produced after the hydration of OPC and be sped up by the CH hydration product and chemical activators. With the prolonging of hydration time, more hydration products such as C-S-H gels and C-A-S-H gels generate, hence causing the great increase of long-term UCS of the SR samples. This result is consistent with the findings of Obuzor et al. [40]. Therefore, the utilization of the low-alkalinity binder to solidify total gold tailing can greatly improve long-term strength and work efficiency.

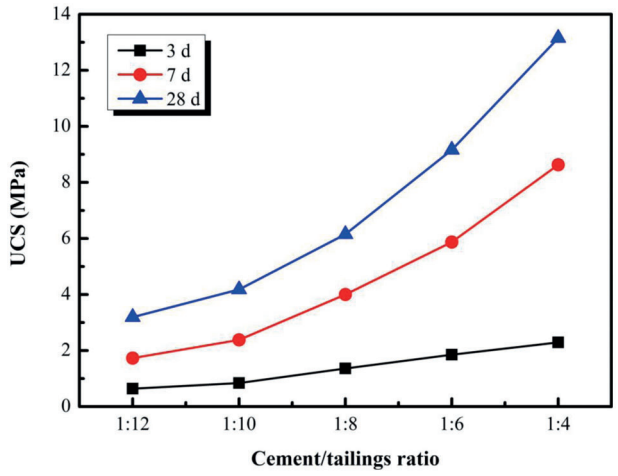

Figure 6: Effect of cement/tailings ratio on the UCS value of the SR samples

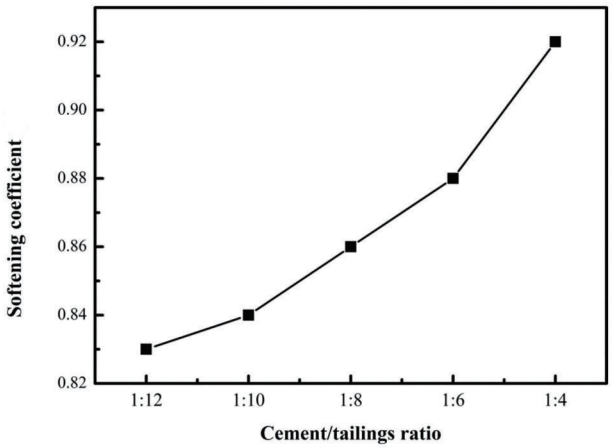

Figure 7: Effect of cement/tailings ratio on the softening coefficient of the SR samples

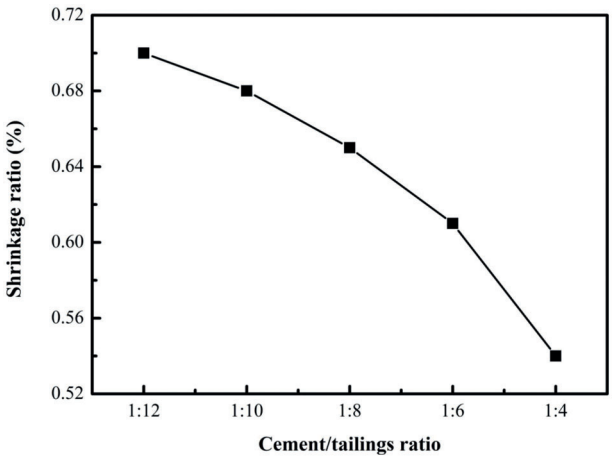

Figure 8: Effect of cement/tailings ratio on the shrinkage ratio of the SR samples at 28 d curing age

Table 7: 3 and 7 d compressive strength growth rates of the SR samples

Cement/tailings ratio	3 d strength growth rate/%	7 d strength growth rate/%
1:4	17.4	65.6
1:6	20.2	64.1
1:8	22.1	65.0
1:10	20.1	56.9
1:12	20.1	54.2

Li et al. [41] developed a new filling cementitious material using blast furnace slag, quick lime, mirabilite, and inorganic salt as cementing components to bind total tailings and found a ration optimization of 73.8% slag, 8% semi-hydrated gypsum, 6% lime, 1.2% mirabilite, 0.6% NaCl, and 0.4% $CaCl_2$. When the solid content and the cement/tailing ratio are 70 wt% and 1:8, the 28 d filling-body strength is 2.87 MPa, which lowers the experimental result obtained by the BLA binder. The UCS values

of the SR samples with 1:8, 1:6, and 1:4 cement/tailing ratios can completely meet the requirements of this mining plant ($UCS_{3\ d} \geq 0.5$ MPa, $UCS_{7\ d} \geq 1.0$ MPa, $UCS_{28\ d} \geq 2.0$ MPa).

However, the recommended cement/tailings ratio is 1:6 in this study by synthesizing the factors of economy and engineering reliability. In the binder of BLA, the OPC:GBFS:FA ratio is 3:6:1, showing that the content of solid wastes in the CPB accounts for about 70 wt%. The calculated mass fraction of GBFS and FA is merely approximately 7.3 wt% as the solid content is 70 wt%. If 700 thousand tons total tailings are produced annually for a given gold mine, then 73 thousand tons GBFS and FA will be consumed. This result obtained in our current work offers an effective strategy for the recycling of GBFS and FA and the reduction in cement consumption.

As shown in Fig. 7, the softening coefficient increases continuously when the cement/tailings ratio increases. As the cement/tailing ratio is 1:12, the softening coefficient of the SR samples is greater than 0.80, and the softening coefficient exceeds 0.90 when the cement/tailing ratio is 1:4. These data indicate that the cementing backfill materials with BLA have good water resistance. The C-S-H gels and C-A-S-H gels produced in the hydration reactions of the cement and GBFS can fill the voids and cement the fine tailings particles together into an integrated whole by consuming the water in the CPB slurry. When the amount of the binder in the CPB slurry is inadequate (low cement/tailings ratio such as 1:10 and 1:12), the reduced C-S-H gels and C-A-S-H gels cannot cement the fine tailings particles, leading to the decrease in the softening coefficient.

As can be seen from Fig. 8, when the cement/tailings ratio increases, the shrinkage ratio decreases continuously, showing an opposite trend to the softening coefficient. All the shrinkage ratio values are relatively low (less than 0.7%) in the investigated cement/tailings ratio range. Low shrinkage can make the sample keep intact shape and is not easy to crack it during curing period.

3.4 Effects of Solid Content on the Performances of CPB

The effect of solid content on the strength evolution of the SR samples for curing times of 3, 7, and 28 d is shown in Fig. 9. As can be seen in this figure, an increase in the tailing slurry solid content leads to an improvement in the UCS irrespective of the curing time of the SR samples. Only the increasing degree of the 3 d UCS is relatively low. For example, with an increase in the solid content from 60 wt% to 70 wt%, the UCS of the SR samples increases from 1.36 to 1.85 MPa (0.49 MPa increment), whereas those of the SR samples at 7 and 28 d curing age increase from 3.55 to 5 MPa (1.45 MPa increment) and from 4.57 to 8.25 MPa (3.68 MPa increment), respectively. The results of the UCS evolutions also give corresponding evidence, as marked in Fig. 8. Higher solid content remarkably improves the UCS of the SR samples.

In the investigated solid contents, the strength evolution relationship between the UCS and the tailings slurry solid content shows a similar tendency: relatively lower 3 d UCS value, rapidly increased 7 d UCS value, and highest 28 d UCS value. Prolonging curing time allows more time for the hydration of OPC and GBFS in the BLA binder, thereby generating more hydration products. It is noteworthy that the 60 wt% solid content is inappropriate to use in the underground mine filling although the UCS values of the SR samples with different curing ages meet the requirements of underground mine filling. Lower solid content always results in excessive fluidity and hence reduces stability of filling slurry.

3.5 Effects of Tailings Fineness on the UCS of CPB

Generally, in the total dried mass of CPB, the mass fraction of the tailings exceeds 70 wt%. Hence, the effect of tailings performances such as density, chemical component, fineness on the performance of CPB cannot be overlooked. Tailings fineness is an important factor affecting the performance of CPB due to its variability caused by mineral processing methods and mineralogical composition. Herein, the effect of

tailings fineness, which is represented by three tailings types of TT, FT, and CT, on the UCS of the ST samples was studied. As indicated in Table 8, no observable 3 d UCS is obtained for the CPB adding 0.15 wt% superplasticizer and using CT as raw materials. We found that their early-term strengths are so weak that cannot demould because the addition of superplasticizer can lead to the segregation and dewatering of the coarse tailings slurry. When the superplasticizer is not added, the 3 d UCS of the hardened samples with CT can be achieved while the 7 and 28 d UCS values decrease.

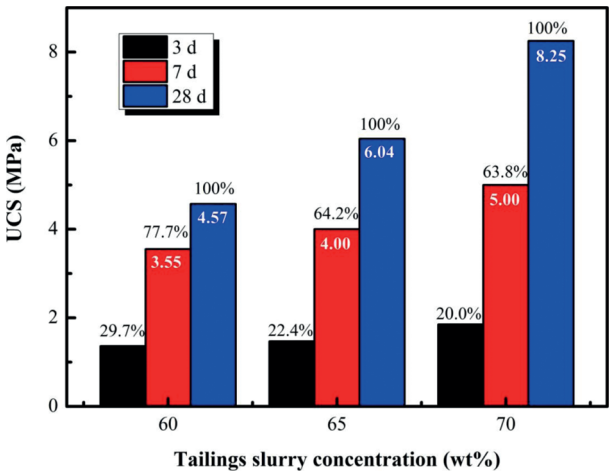

Figure 9: Effect of solid content on the strength evolution of the SR samples for curing times of 3, 7 and 28 d

Table 8: 3 d UCS of the ST samples

Tailings fineness	Cement/tailings ratio	Superplasticizer content (wt%)	Solid content (wt%)	3 d UCS/MPa
TT	1:6	0.15	65	1.47
FT	1:6	0.15	65	1.88
CT	1:6	0.15	65	—
CT	1:6	—	65	0.94

Fig. 10 depicts the influence of tailings fineness on the UCS of the ST samples at 7 and 28 d curing ages. It is revealed from the report of Fall et al. that the tailings fineness has a remarkable influence on the strength of the CPB [42]. The ST samples with TT exhibit the highest 7 and 28 d UCS, which indicates that over-coarse or over-fine average particle size is detrimental to the improvement of the UCS of the CPB with BLA. Our investigation seems to contradict the findings of Fall et al. [42]. In their investigation, they found that coarse and medium tailings are more advantageous to achieve good mechanical strength. The result obtained in our current work agrees well with the investigation of Ke et al. [43]. These different results may be derived from the variation of paste film thickness, which has been proved by several studies [44–46]. That is, a slightly higher UCS of the CPB can be gained when the tailings fineness is higher than 54.42%. As mentioned above, the proportions of the fine particles with less than 20 μm in TT and FT are 72.1% and 81.5%, respectively. At present, the utilization rate of fine gold tailings in China and other developed countries is considerably lower than that of coarse gold tailings. Therefore, under this background, it is exciting and significant to apply the BLA developed successfully by our group to fabricate CPB for bulk utilization of fine gold tailings.

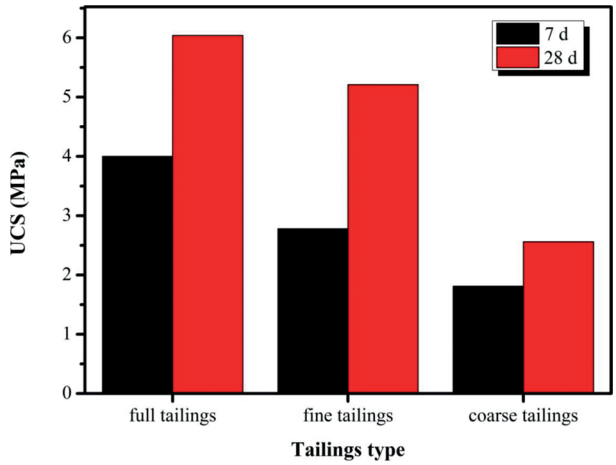

Figure 10: Effect of tailings fineness on the UCS of the ST samples at 7 and 28 d curing ages

3.6 XRD and SEM Analysis of the CPB Samples

Fig. 11 shows the XRD patterns of the TT and the SR sample after curing for 28 d. As seen in Fig. 11a, the main mineral phase is quartz (SiO_2) for the total gold tailings, which is in accordance with the XRF result. Small amount of anorthite phase ($CaAl_2Si_2O_8$) is also observed in the Fig. 11a, revealing that the gold tailings used in our work can be classified as felsic-type tailings. For the SR sample with 28 d curing age, as revealed in Fig. 11b, except quartz, some primary hydration products derived from the hydration reaction of BLA such as C-S-H gels, C-A-S-H gels, and afwillite ($C_3S{\cdot}yH_2O$) are detected. According to the report of Lodeiro [47], Al^{3+} can enter the C-S-H structure to replace Si^{2+} in the silicon-oxygen tetrahedra, increasing the degree of polymerization of the silicon-oxygen tetrahedra. The presence of a certain amount of Al^{3+} in CPB can result in the formation of a certain amount of C-A-S-H. These hydration products are the main sources of strength and can notably improve the engineering properties of CPB. In particular, the C-A-S-H gels with tobermorite structure are easily generated in alkali-activated compositions and they can present network cross-connections, providing the samples with good performances as compared with hydrated cement with C-S-H networks [28,29].

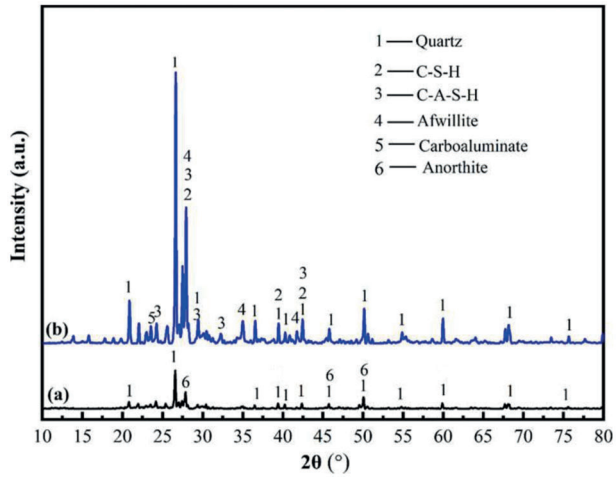

Figure 11: XRD patterns of the TT (a) and the SR sample after curing for 28 d (b)

Fig. 12 displays the SEM images magnified 500 times and 2000 times of the CPB specimens using BLA and OPC as binders, respectively. Compared with Figs. 12c and 12d, the CPB specimen with BLA exhibits a relatively dense microstructure without virtual gaps. Clearly, the hydration products generated in the hydration and hardening process are close together. Correspondingly, the voids between gold tailings particles are filled by ultrafine FA in BLA binder and these hydration products. The reduced porosity of hardened cement-based materials is a crucial factor for obtaining high UCS and good durability.

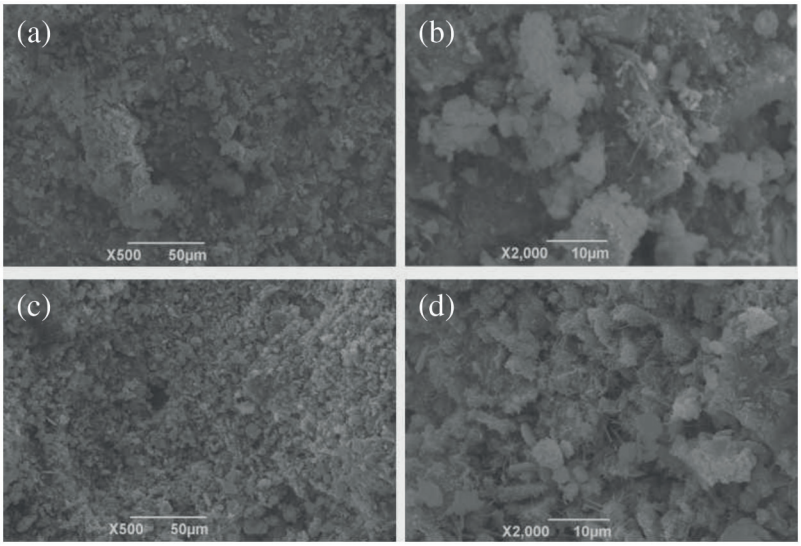

Figure 12: SEM images of the CPB specimens using BLA and OPC as binders, respectively: (a) and (b), BLA; (c) and (d), OPC

It is well known that the raw materials OPC, GFBS, and FA have a similar chemical composition mainly including CaO, SiO_2, and Al_2O_3. In particular, the OPC clinker is composed of C_3S, C_2S, and C_3A. A large number of C-S-H and C-H will be produced as the hydration reactions of C_3S and C_2S occur according to the Eqs. (4) and (5):

$$3CaO \cdot SiO_2 + nH_2O \rightarrow xCaO \cdot SiO_2 \cdot yH_2O + (3 - x)Ca(OH)_2 \quad (4)$$

$$2CaO \cdot SiO_2 + nH_2O \rightarrow xCaO \cdot SiO_2 \cdot yH_2O + (2 - x)Ca(OH)_2 \quad (5)$$

Meanwhile, the hydration of lime (CaO) in the CPB can also produce a certain amount of calcium hydroxide. However, several pores will generate, which is greatly detrimental to the UCS [48]. In the calcium hydroxide solution, the vitreous structure of GBFS is destroyed and the pozzolanic activity of GBFS can be inspired. Moreover, the sodium sulfate in the BLA can further stimulate its pozzolanic activity based on the alkali excitation effect. As a result, signification hydrations occur according to the following equations:

$$xCa(OH)_2 + SiO_2 + mH_2O \rightarrow xCaO \cdot SiO_2 \cdot yH_2O \quad (6)$$

$$xCa(OH)_2 + Al_2O_3 + mH_2O \rightarrow xCaO \cdot Al_2O_3 \cdot yH_2O \quad (7)$$

Correspondingly, calcium hydroxide is consumed and amorphous hydrated calcium (aluminum) silicate is formed. After a long time period, microcrystalline or crystalline calcium (aluminum) silicate gels are finally transformed. The stability and compactness of these produced C-S-H gels and C-A-S-H gels are higher than C-H. The resulting hydration products can fill in the pores and cement tailings particles.

Finally, the compact structure is obtained and the strength of the samples is improved. Therefore, the BLA is a favorable binder for the CPB by tailoring the pore structure distribution and participating in the secondary hydration reaction.

4 Conclusions

The purpose of the investigation in this work was to explore the practicability of applying a mixture low-alkalinity binder to produce cemented paste backfill (CPB). The influencing factors on the engineering and microstructural performances of the CPB were analyzed in detail using the single factor experiment. Based on the experimental results and discussion, the following conclusions can be drawn:

1. Compared with the specimens using OPC as binder alone, the UCS value of the specimens with BLA was increased sharply, which should be attributed to the partial replacement of OPC by GBFS and FA. Although the addition of BLA remarkable lowered the slump values, all of them were acceptable to meet the fluidity requirements of the Zhaoyuan gold mine.
2. The slump value increased from 260 to 290 mm when the superplasticizer dosage increased from 0 wt% to 0.20 wt%. The UCS value of the CPB specimens increased gradually as the superplasticizer content increased from 0 wt% to 0.15 wt%, and decreased at 0.20 wt% superplasticizer content regardless of curing age.
3. The strength evolution relationship between the UCS and the solid content showed a similar tendency: relatively lower 3 d UCS value, rapidly increased 7 d UCS value, and highest 28 UCS value. Over-coarse or over-fine average particle size was detrimental to the improvement of the UCS of the CPB with BLA.
4. The BLA was proved to be a promising binder to improve the engineering performances of the CPB. The optimal mixing ratio is 1:6 cement/tailings ratio, 0.15 wt% superplasticizer dosage, and 70 wt% solid content. Prepared by this mixing ratio, the UCS values of the CPB after 3, 7, and 28 d reached 1.85, 5.87, and 9.16 MPa, respectively, which were suitable as the CPB for the Zhaoyuan gold mine in terms of strength requirements.

Funding Statement: The current work was financially supported by the Key Research and Development Program of Anhui Province (202004a07020039).

Conflicts of Interest: The authors declare that they have no conflicts of interest to report regarding the current study.

References

1. Lyu, X. J., Yao, G., Wang, Z. M., Wang, Q., Li, L. (2020). Hydration kinetics and properties of cement blended with mechanically activated gold mine tailings. *Thermochimica Acta, 683,* 178457. DOI 10.1016/j.tca.2019.178457.
2. Lu, H. J., Qi, C. C., Chen, Q. S., Gan, D. Q., Xue, Z. L. et al. (2018). A new procedure for recycling waste tailings as cemented paste backfill to underground stopes and open pits. *Journal of Cleaner Production, 188(12),* 601–612. DOI 10.1016/j.jclepro.2018.04.041.
3. Sun, W., Wang, H., Hou, K. (2018). Control of waste rock-tailings paste backfill for active mining subsidence areas. *Journal of Cleaner Production, 171,* 567–579. DOI 10.1016/j.jclepro.2017.09.253.
4. Wang, Y., Chen, L. H. (2020). Comprehensive utilization of a gold mine tailings and preliminary analysis of reclaimed soil with secondary tailings. *Hunan Nonferrous Metals, 36(1),* 11–14 (in Chinese). DOI 10.3969/j.issn.1003-5540.2020.01.004.
5. Ai, Y. J., Li, F. P., Gu, H. H., Chi, X. J., Yuan, X. T. et al. (2020). Combined effects of green manure returning and addition of sewage sludge compost on plant growth and microorganism communities in gold tailings. *Environmental Science and Pollution Research, 27(25),* 31686–31698. DOI 10.1007/s11356-020-09118-z.

6. Li, H. Y., Peng, J. H., Long, H. L., Li, S. W., Zhang, L. B. (2021). Cleaner process: Efficacy of chlorine in the recycling of gold from gold containing tailings. *Journal of Cleaner Production, 287(9),* 125066. DOI 10.1016/j.jclepro.2020.125066.
7. Rodrigues, M. L. M., Giardini, R. M. N., Pereira, I. J. U. V., Leão, V. A. (2021). Recovering gold from mine tailings: A selection of reactors for bio-oxidation at high pulp densities. *Journal of Chemical Technology and Biotechnology, 96(1),* 217–226. DOI 10.1002/jctb.6530.
8. Calderon, A. R. M., Alorro, R. D., Tadesse, B., Yoo, K., Tabelin, C. B. (2020). Repurposing of nickeliferous pyrrhotite from mine tailings as magnetic adsorbent for the recovery of gold from chloride solution. *Resources Conservation and Recycling, 161(12–13),* 104971. DOI 10.1016/j.resconrec.2020.104971.
9. Guo, X. Y., Qin, H., Tian, Q. H., Zhang, L. (2020). The efficacy of a new iodination roasting technology to recover gold and silver from refractory gold tailing. *Journal of Cleaner Production, 261(2),* 121147. DOI 10.1016/j.jclepro.2020.121147.
10. Mashifana, T., Sebothoma, J., Sithole, T. (2021). Alkaline activation of basic oxygen furnace slag modified gold mine tailings for building material. *Advances in Civil Engineering, 2021(1),* 9984494. DOI 10.1155/2021/9984494.
11. Wang, Q., Li, J. J., Zhu, X. N., Yao, G., Wu, P. et al. (2020). Approach to the management of gold ore tailings via its application in cement production. *Journal of Cleaner Production, 269(3),* 122303. DOI 10.1016/j.jclepro.2020.122303.
12. Wang, Q., Yao, G., Zhu, X. N., Wang, J. X., Wu, P. et al. (2019). Preparation of Portland cement with gold ore tailings. *Advances in Materials Science and Engineering, 2019,* 1324065. DOI 10.1155/2019/1324065.
13. Chen, W. Q., Li, Y. H., La, P. Q., Xue, Y. Q., Li, Z. P. et al. (2021). Influences of thermal treatment temperature on microstructures and properties of glass-ceramics from gold tailings. *Ferroelectrics, 579(1),* 23–32. DOI 10.1080/00150193.2021.1903264.
14. Wei, Z. A., Zhao, J. K., Wang, W. S., Yang, Y. H., Zhuang, S. N. et al. (2021). Utilizing gold mine tailings to produce sintered bricks. *Construction and Building Materials, 282(4),* 122655. DOI 10.1016/j.conbuildmat.2021.122655.
15. Yilmaz, E., Belem, T., Bussière, B., Mbonimpa, M., Benzaazoua, M. (2015). Curing time effect on consolidation behaviour of cemented paste backfill containing different cement types and contents. *Construction and Building Materials, 75(2),* 99–111. DOI 10.1016/j.conbuildmat.2014.11.008.
16. Xu, W. B., Chen, W., Tian, M. M., Guo, L. J. (2021). Effect of temperature on time-dependent rheological and compressive strength of fresh cemented paste backfill containing flocculants. *Construction and Building Materials, 267(4),* 121038. DOI 10.1016/j.conbuildmat.2020.121038.
17. Zhao, Y., Taheri, A., Karakus, M., Chen, Z. W., Deng, A. (2020). Effects of water content, water type and temperature on the rheological behaviour of slag-cement and fly ash-cement paste backfill. *International Journal of Mining Science and Technology, 30(3),* 271–278. DOI 10.1016/j.ijmst.2020.03.003.
18. Koohestani, B., Belem, T., Koubaa, A., Bussière, B. (2016). Experimental investigation into the compressive strength development of cemented paste backfill containing nano-silica. *Cement & Concrete Composites, 72(10),* 180–189. DOI 10.1016/j.cemconcomp.2016.06.016.
19. Fridjonsson, E. O., Hasan, A., Fourie, A. B., Johns, M. L. (2013). Pore structure in a gold mine cemented paste backfill. *Mineral Engineering, 53(257),* 144–151. DOI 10.1016/j.mineng.2013.07.017.
20. Kou, Y. P., Jiang, H. Q., Ren, L., Yilmaz, E., Li, Y. H. (2020). Rheological properties of cemented paste backfill with alkali-activated slag. *Minerals, 10(3),* 288. DOI 10.3390/min10030288.
21. Thabo, F., Freeman, N., Felix, O. (2018). Synthesis of a paste backfill geopolymer using pure acidic gold mine tailings. *Journal of Solid Waste Technology and Management, 44(4),* 311–320. DOI 10.5276/JSWTM.2018.311.
22. Yilmaz, E., Benzaazoua, M., Belem, T., Bussiere, B. (2009). Effect of curing under pressure on compressive strength development of cemented paste backfill. *Mineral Engineering, 22(9–10),* 772–785. DOI 10.1016/j.mineng.2009.02.002.
23. Ercikdi, B., Cihangir, F., Kesimal, A., Deveci, H., Alp, I. M. (2010). Utilization of water-reducing admixtures in cemented paste backfill of sulphide-rich mill tailings. *Journal of Hazardous Materials, 179(1–3),* 940–946. DOI 10.1016/j.jhazmat.2010.03.096.

24. Ercikdi, B., Kesimal, A., Cihangir, F., Deveci, H., Alp, I. (2009). Cemented paste backfill of sulphide-rich tailings: Importance of binder type and dosage. *Cement & Concrete Composites, 31(4),* 268–274. DOI 10.1016/j.cemconcomp.2009.01.008.
25. Fall, M., Pokharel, M. (2010). Coupled effects of sulphate and temperature on the strength development of cemented tailings backfills: Portland cement-paste backfill. *Cement & Concrete Composites, 32(10),* 819–828. DOI 10.1016/j.cemconcomp.2010.08.002.
26. Chen, C. L., Li, X. J., Chen, X. D., Chai, J. H., Tian, H. X. (2019). Development of cemented paste backfill based on the addition of three mineral additions using the mixture design modeling approach. *Construction and Building Materials, 229(3),* 116919. DOI 10.1016/j.conbuildmat.2019.116919.
27. Cao, S., Song, W. D., Yilmaz, E. (2018). Influence of structural factors on uniaxial compressive strength of cemented tailings backfill. *Construction and Building Materials, 174(8),* 190–201. DOI 10.1016/j.conbuildmat.2018.04.126.
28. Marvila, M. T., Azevedo, A. R. G., Matos, P. R., Monteiro, S. N., Vieira, C. M. F. (2021). Rheological and the fresh state properties of alkali-activated mortars by blast furnace slag. *Materials, 14,* 2069. DOI 10.3390/ma14082069.
29. Marvila, M. T., Azevedo, A. R. G., Oliveira, L. B., Xavier, G. C., Vieira, C. M. F. (2021). Mechanical, physical and durability properties of activated alkali cement based on blast furnace slag as a function of $\%Na_2O$. *Construction and Building Materials, 15,* e00723. DOI 10.1016/j.cscm.2021.e00723.
30. Li, J., Zhang, S. Q., Wang, Q., Ni, W., Li, K. Q. et al. (2020). Feasibility of using fly ash-slag-based binder for mine backfilling and its associated leaching risks. *Journal of Hazardous Materials, 400,* 123191. DOI 10.1016/j.jhazmat.2020.123191.
31. He, Y., Chen, Q. S., Qi, C. C., Zhang, Q. L., Xiao, C. C. (2019). Lithium slag and fly ash-based binder for cemented fine tailings backfill. *Journal of Environmental Management, 248(4),* 109282. DOI 10.1016/j.jenvman.2019.109282.
32. Chen, Q. S., Zhang, Q. L., Fourie, A., Xin, C. (2017). Utilization of phosphogypsum and phosphate tailings for cemented paste backfill. *Journal of Environmental Management, 201(1),* 19–27. DOI 10.1016/j.jenvman.2017.06.027.
33. Zhang, S. Y., Zhao, Y. L., Ding, H. X., Qiu, J. P., Hou, C. (2021). Effect of sodium chloride concentration and pre-curing time on the properties of cemented paste backfill in a sub-zero environment. *Journal of Cleaner Production, 283(3),* 125310. DOI 10.1016/j.jclepro.2020.125310.
34. Sun, Q., Li, T. L., Liang, B. (2020). Preparation of a new type of cemented paste backfill with an alkali-activated silica fume and slag composite binder. *Materials, 13(2),* 372. DOI 10.3390/ma13020372.
35. Ercikdi, B., Cihangir, F., Kesimal, A., Deveci, H., Alp, I. (2009). Utilization of industrial waste products as pozzolanic material in cemented paste backfill of high sulphide mill tailings. *Journal of Hazardous Materials, 168(2–3),* 848–856. DOI 10.1016/j.jhazmat.2009.02.100.
36. Zheng, J. R., Tang, Y., Feng, H. (2021). Utilization of low-alkalinity binders in cemented paste backfill from sulphide-rich mine tailings. *Construction and Building Materials, 290(10),* 123221. DOI 10.1016/j.conbuildmat.2021.123221.
37. Hou, Y. B., Wei, S. X., Wang, B. W. (2016). *Technology of the emission of cement tailings*. China: Metallurgical Industry Press (in Chinese).
38. Khaldoun, A., Ouadif, L., Baba, K., Bahi, L. (2016). Valorization of mining waste and tailings through paste backfilling solution, Imiter operation. *Morocco International Journal of Mining Science and Technology, 26(3),* 511–516. DOI 10.1016/j.ijmst.2016.02.021.
39. Qi, C. C., Chen, Q. S., Fourie, A., Zhao, J. W., Zhang, Q. L. (2018). Pressure drop in pipe flow of cemented paste backfill: Experimental and modeling study. *Powder Technology, 333,* 9–18. DOI 10.1016/j.powtec.2018.03.070.
40. Obuzor, G. N., Kinuthia, J. M., Robinson, R. B. (2011). Enhancing the durability of flooded low-capacity soils by utilizing lime-activated ground granulated blast furnace slag (GGBS). *Engineering Geology, 123(3),* 179–186. DOI 10.1016/j.enggeo.2011.07.009.
41. Li, L. T., Yang, Z. Q., Gao, Q. (2018). Ration optimization of new filling cementitious material based on orthogonal test and neural network model. *Multipurpose Utilization of Mineral Resources, 3,* 114–120 (in Chinese). DOI 10.3969/j.issn.1000-6532.2018.03.024.

42. Fall, M., Belem, T., Samb, S., Benzaazoua, M. (2007). Experimental characterization of the stress-strain behaviour of cemented paste backfill in compression. *Journal of Materials Science, 42(11),* 3914–3922. DOI 10.1007/s10853-006-0403-2.
43. Ke, X., Hou, H., Zhou, M., Wang, Y., Zhou, X. (2015). Effect of particle gradation on properties of fresh and hardened cemented paste backfill. *Construction and Building Materials, 96,* 378–382. DOI 10.1016/j.conbuildmat.2015.08.057.
44. Kwan, A. K. H., Li, L. G. (2012). Combined effects of water film thickness and paste film thickness on rheology of mortar. *Materials and Structure, 45(9),* 1359–1374. DOI 10.1617/s11527-012-9837-y.
45. Zheng, J., Zhu, Y., Zhao, Z. (2016). Utilization of limestone powder and water-reducing admixture in cemented paste backfill of coarse copper mine tailings. *Construction and Building Materials, 124,* 31–36. DOI 10.1016/j.conbuildmat.2016.07.055.
46. Kwan, A. K. H., Li, L. G. (2014). Combined effects of water film, paste film and mortar film thicknesses on fresh properties of concrete. *Construction and Building Materials, 50(10),* 598–608. DOI 10.1016/j.conbuildmat.2013.10.014.
47. Lodeiro, I. G., Jimenez, A. F., Palomo, A., Macphee, D. E. (2010). Effect on fresh C-S-H gels of the simultaneous addition of alkali and aluminium. *Cement and Concrete Research, 40(1),* 27–32. DOI 10.1016/j.cemconres.2009.08.004.
48. Cihangir, F., Ercikdi, B., Kesimal, A., Ocak, S., Akyol, Y. (2018). Effect of sodium-silicate activated slag at different silicate modulus on the strength and microstructural properties of full and coarse sulphidic tailings paste backfill. *Construction and Building Materials, 185,* 555–566. DOI 10.1016/j.conbuildmat.2018.07.105.